JARO 14: 3–15 (2013)
DOI: 10.1007/s10162-012-0355-y

JARO
Journal of the Association for Research in Otolaryngology

Research Article

Decellularized Ear Tissues as Scaffolds for Stem Cell Differentiation

Peter A. Santi[1] and Shane B. Johnson[1]

[1]*Department of Otolaryngology, University of Minnesota, Lions Research Building, 2001 Sixth Street, SE, Minneapolis, MN 55455, USA*

Received: 4 May 2012; Accepted: 2 October 2012; Online publication: 20 October 2012

ABSTRACT

Permanent sensorineural hearing loss is a major medical problem and is due to the loss of hair cells and subsequently spiral ganglion neurons in the cochlea. Since these cells lack the capacity of renewal in mammals, their regeneration would be an optimal solution to reverse hearing loss. In other tissues, decellularized extracellular matrix (ECM) has been used as a mechanical and biochemical scaffold for the induction of stem and other cells toward a target tissue phenotype. Such induced cells have been used for tissue and organ transplants in preclinical animal and human clinical applications. This paper reports for the first time the decellularization of the cochlea and identification of remaining laminin and collagen type IV as a first step in preparing an ECM scaffold for directing stem cells toward an auditory lineage. Fresh ear tissues were removed from euthanized mice, a rat and a human and processed for decellularization using two different detergent extraction methods. Cochleas were imaged with scanning thin-sheet laser imaging microscopy (sTSLIM) and brightfield microscopy. Detergent treatment of fresh tissue removed all cells as evidenced by lack of H&E and DNA staining of the membranous labyrinth while preserving components of the ECM. The organ of Corti was completely removed, as were spiral ganglion neurons, which appeared as hollow sheaths and tubes of basal lamina (BL) material. Cells of the stria vascularis were removed and its only vestige left was its laterally linking network of capillary BL that appeared to "float" in the endolymphatic space. Laminin and type IV collagen were detected in the ECM after decellularization and were localized in vascular, neural and epithelial BL. Further work is necessary to attempt to seed neural and other stem cells into the decellularized ECM to hopefully induce differentiation and subsequent in vivo engraftment into damaged cochleas.

Keywords: tissue engineering, decellularization, extracellular matrix, cochlea, vestibular, stem cells

INTRODUCTION

Sensorineural hearing loss (SNHL) is a major medical problem that affects millions of people worldwide. It is due to the failure of hair cells and spiral ganglion neurons to regenerate after damage to the mammalian cochlea. Hair cell and nerve cell regeneration would be the optimal solution to reverse SNHL, and efforts to accomplish this task can be divided into two strategies. Gene therapy methods, such as stimulation of Atoh1 (Izumikawa et al. 2005), disruption of Notch signaling (Hori et al. 2007), and targeted deletion of p27Kip1 (Löwenheim et al. 1999) which have resulted in production of supernumerary hair and supporting cells. However, these gene-based strategies face significant challenges to produce the correct number, placement, and functional recovery of cells. Another strategy is to induce differentiation of stem cells toward an auditory neuronal lineage in vitro using neurotrophins, BMP4, and conditioned media (Nayagam and Minter 2011). When conditioned neural progenitor cells, derived from embryonic stem cells, were injected into the VIII nerve of denervated cochleas, the cells implanted and extended nerve fibers to the organ of Corti (Corrales et al. 2006).

Correspondence to: Peter A. Santi · Department of Otolaryngology · University of Minnesota · Lions Research Building, 2001 Sixth Street, SE, Minneapolis, MN 55455, USA. Telephone: (612) 626-6800; Fax: (612) 626-5009; e-mail: psanti@umn.edu

Spiral ganglion neurons obtained from newborn mice also grew toward and created synaptic connections with, hair cells in denervated organ of Corti preparations (Martinez-Monedero et al. 2006). In other experiments, NSCs and other stem cells, injected into other parts of the cochlea either remained in the perilymphatic space, expressed glial cell proteins (Iguchi et al. 2003) or in worse case, formed tumors (Lang et al. 2008; Kesser and Lalwani 2009). These initial experiments suggest that the cochlea is amenable in vivo to stem cell migration, proliferation, and differentiation; however, it has yet to be determined whether these cells can make functional peripheral and central connections. Oshima et al. (2010) suggest that it would be beneficial to lead exogenous stem cells along a hair cell (or spiral ganglion cell) pathway by exposing them to cochlear signals in vitro before injection. Toward this goal, the present study produced decellularized cochlear tissue that may be used to direct stem cells to an auditory lineage for transplantation.

The extracellular matrix (ECM) provides structural support, cell adhesion and it plays a vital role in the determination, differentiation, proliferation, survival, polarity, and migration of cells (Hynes 2009). Recent breakthrough technology using decellularized matrix as a scaffold for stem and other progenitor cell differentiation has shown successful engraftment and functional recovery in vivo in several organs, including the heart (Ott et al. 2008), lung (Petersen et al. 2010), trachea (Baiguera et al. 2010) and nerve (Nagao et al. 2011). These studies demonstrate that the native decellularized matrix expresses inductive cues that can direct the differentiation of stem cells towards specific lineages. The mechanisms that mediate this directed differentiation may involve unique sulfation patterns found on glycosaminoglycans (Khan et al. 2008) in an organ and region-specific manner that constitute part of the matrix. Evans et al. (2007) showed that laminin and fibronectin provided guidance cues to neonatal (P5) spiral ganglion neurons using stripe micro-patterns. They further stated that laminin may provide neurite guidance toward the organ of Corti and fibronectin of the basilar membrane may provide a stop or avoidance signal for neurite growth.

A large number of different procedures have been developed for decellularizing tissues and organs for the purpose of organ transplantation. Biological scaffolds obtained from decellularization results in a complex mixture of three-dimensional (3D) structural and functional components of the ECM. It should be noted that each of the different decellularization process alters the ECM and its components; however, the goal is for complete removal of the cells and their cytoplasmic components with minimal structural and compositional disruption of the ECM. Decellularization methods include: various chemical treatments (e.g., acids, bases, hypertonic, hypotonic, detergents, EDTA, and alcohols), enzymatic digestion, and physical agents (freeze/thaw cycles) as reviewed by Gilbert et al. (2006) and Crapo et al. (2011). We have selected two different detergent-based decellularization protocols for producing acellular inner ears. They were chosen for their completeness in decellularization and maintenance of the ECM as described in previous experiments. The first was developed for the heart (Ott et al. 2008) and uses the strong anionic detergent sodium dodecyl sulfate (SDS). The second procedure uses a less strong anionic detergent sodium deoxycholate (SDOC), which has been reported to better preserve ECM components (Erdbrügger 2006). Successful decellularization of cochlear tissues may not only provide a new systems-based approach for cochlear cell regeneration, but it may provide important, new information on the functional anatomy of the cochlea. In this paper, we will describe cochlear morphology after decellularization and show that this procedure is a novel way to separate and harvest cochlear tissues for further anatomical and functional investigation.

METHODS

Animals

Four-week-old CBA/J mice were anesthetized with ketamine/xyzaline and decapitated. Bullae were removed and the cochlea and portions of the middle ear and vestibular system were exposed by microdissection. In total, 45 cochleas were used in this study and ~6,500 histological and optical sections were produced and analyzed. Ten cochleas were fixed by immersion in 4 % paraformaldehyde in PBS overnight at 4 °C. The following day the cochleas were rinsed in PBS (three times, 30 min each) then decalcified (see below). For cochleas intended for decellularization (35), the stapes was dislocated from the oval window and the round window membrane was punctured using a thin polypropylene strand. The perilymphatic scalae were slowly (over 2 min) perfused with 5 ml of either of two different decellularization detergents containing either 1 % SDS in deionized water at room temperature (Ott et al. 2008) or 1 % SDOC in PBS at 37 °C (Erdbrügger et al. 2006). All tissue preparation steps were performed in 20-ml scintillation vials (one cochlea per vial) on a rotator. Tissues were immersed in the decellularization solutions for up to 3 days with daily solution changes and perilymphatic perfusions. In addition, a 6-week-old rat (Sprague Dawley) was also

processed for scanning thin-sheet laser imaging microscopy (sTSLIM) imaging after SDS decellularization as described above for mice. Furthermore, two human temporal bones were used in this study. One was a cellularized, formalin-fixed, decalcified, and cleared human temporal bone and the other was a decellularized temporal bone to compare with our findings in rodents. Animal care and use of the mice in this study was approved by the University of Minnesota IACUC and care was administered by Research Animal Resources. Rat tissue was obtained from a euthanized animal whose care and use was also approved by the University of Minnesota IACUC. Extraction of the human temporal bone was approved by the University of Minnesota Human Subjects Committee.

After 3 days in the decellularization solution with daily perilymphatic perfusions, tissues were rinsed (three changes, 30 min each) in deionized water. Tissues were decalcified by immersion in a 10 % solution (pH 7.3) of EDTA in deionized water for 3 days daily solution changes. After several 2-h PBS washes, decalcified ears were dehydrated in an ascending ethanol series and stained for 24 h with Rhodamine B isothiocyanate in 100 % ethanol, which behaves like a general fluorescent stain analogous to eosin in brightfield microscopy. Stained tissues were then cleared with a 5:3 mixture of methyl salicylate to benzyl benzoate (MSBB) until transparent and mounted for sTSLIM (Santi et al. 2009; Schröter et al. 2012). The human temporal bone was removed fresh without fixation and immediately placed in SDS for 15 days in total, with solution changes every day. Both human temporal bones were trimmed down to the level of the cochlea, decalcified, cleared in MSBB, and imaged with TSLIM and sTSLIM.

sTSLIM

Serial optical sections of the whole cochlea were imaged using our sTSLIM device, which has been previously described (Santi et al. 2009; Schröter et al. 2012). Briefly, whole, chemically cleared cochleas were mounted onto a specimen rod and placed in an open top, glass fluorometer cell (Starna Cells, Atascadero, CA) in the sTSLIM device. The specimen rod could rotate 360° and move in the *x*-, *y*-, and *z*-axes using motorized micropositioners (Newport, Irvine, CA) that were driven using a custom LabVIEW (National Instruments, Austin, TX) program interfaced to a Newport controller. For maximum resolution across the width of the cochlea, each optical section was also scanned in the *x*-axis through the beam waist of the light-sheet that was generated using a 532-nm green laser (Meshtel, Geno, NV). A serial stack of optical sections through the midmodiolar plane of the cochlea was collected using the ×1 or ×2 objective of an Olympus microscope (MVX10 MacroView) by moving the specimen in 5-μm steps in the *z*-axis. Due to the size of the cochlea, a complete stack of images consisted of approximately 320 tif files that were 1,600×1,200 pixels in size and were collected using a Retiga 2000R digital camera (Qimaging, Surrey, BC, Canada). Each voxel represented 1.5×1.5×5 μm^3 of tissue volume. Using orthogonal sections, the height of the basilar membrane structures were measured in two animals using the 3D length tool.

Cryosectioning

Decalcified cochleas were rinsed in PBS (three changes, 30 min) then immersed in 30 % sucrose in PBS for 2 h, then placed in OCT overnight. Trapped air was removed under vacuum and blocks were frozen; 15 μm thick sections were cut on a microtome and mounted on polysine slides for staining and imaging.

H&E staining

Hematoxylin and eosin staining was performed as follows: 15 μm cryosections were stained with Harris's hematoxylin solution for 20 min, rinsed with tap water for 5 min, differentiated in 1 % acid alcohol (0.3 % HCl in 70 % ethanol) for 10 s, then rinsed again in tap water for 1 min. Sections were then "blued" in 0.2 % ammonia in tap water for 1 min, rinsed in tap water for 5 min, and dehydrated in 95 % ethanol. After dehydration, the sections were counterstained in eosin Y solution for 5 s followed by three changes of absolute ethanol (5 min each) and were finally cleared in xylene and mounted for imaging.

Immunohistochemistry

For immunohistochemical demonstration of type IV collagen and laminin, whole cochleas that had been decellularized, decalcified, and rinsed in PBS containing a blocking solution (5 % normal goat serum, 0.3 % Triton X-100, and 1 % BSA in PBS) were perfused perilymphatically and immersed in a 1:500 concentration of primary antibody (type IV collagen (Abcam, ab19808) and laminin (Santa Cruz, sc-5584) for 3 days with rotation. After rinsing in PBS, tissues were treated with secondary antibody (1:100 dilution of goat anti-rabbit IgG Alexa Fluor 532 antibody; Invitrogen, A11009) for 3 days with rotation. Tissues were then rinsed in PBS, dehydrated, and cleared for sTSLIM imaging. Antibody-labeled tissues were not counterstained with Rhodamine.

Nuclear staining

For detection of DNA in cell nuclei, SYTOX® orange nucleic acid stain (Invitrogen) was used. Paraformaldehyde-fixed cellularized and fresh, unfixed, decellularized ear tissues were incubated in 5 μM SYTOX® with perilymphatic perfusion, immersion, and rota-

tion for 3 days. Tissues were rinsed in deionized water, dehydrated, and cleared for sTSLIM imaging. All tissues were treated with chemicals in the order specified, and all tissues were treated with EDTA to remove calcium, ethanol to remove water and lipids, and MSBB to remove lipids and clear tissues to transparency.

RESULTS

Whole cochleas were imaged with sTSLIM which resolved connective tissues and cells to a resolution level of the cell nucleolus. sTSLIM midmodiolar cross-sections through a normal cochlea fixed in paraformaldehyde showed the full complement of cells and extracellular connective tissues (Fig. 1A). Detergent treatment of fresh, unfixed cochleas resulted in the complete removal of the cells of the membranous labyrinth of the cochlea and preservation of cochlear ECM (Fig. 1B, C). After decellularization with either detergent, the cochleas became more translucent. SDOC detergent treatment did not appear to extract as much cellular elements (Fig. 1B) as SDS detergent treatment (Fig. 1C). Cell debris were present within the ECM surrounding the spiral ganglion neurons and nerves after SDOC (Fig. 1B) but not after SDS treatment (Fig. 1C), depending upon perfusion and length of immersion. Spiral ganglion neurons appeared as hollow spheres and tubes of basal lamina (BL) material after SDS decellularization. Decellularization was successful only when applied to fresh, unfixed tissues, as exposure of fixed tissue to detergent solutions did not noticeably change cell morphology (not shown). The route of administration and time of exposure of ear tissues to detergents were important factors in the extent of decellularizaton. Due to the extensive fluid-filled spaces of the cochlea, detergents were perfused multiple times through the perilymphatic spaces, rather than through the intravascular route as has been done for the decellularization of other organs (Ott et al. 2008; Petersen et al. 2010). During detergent perfusion through the cochlea, the effluent was cloudy and contained filamentous structures, which presumably were solubilized cell components. Longer incubations (72 h) and frequent perfusions of detergents were necessary to dissolve cell structures that were more tightly surrounded by bone, such as the spiral ganglion neurons within Rosenthal's canal and the nerves in the modiolus. Osteocytes were the only other cells of the cochlea that resisted detergent removal, presumably due to a penetration problem through the dense bone. Details on the effect of decellularization on the cells and tissues of the cochlea are described below.

Higher magnification of the scala media showed details of the decellularization process (Fig. 2A–D). Figure 2A shows a cellularized scala media with the cells of the basilar membrane including the organ of Corti, stria vascularis, Reissner's membrane, spiral ganglion neurons, and nerves. Figure 2B shows the effect of decellularization in SDS for 12 h and without

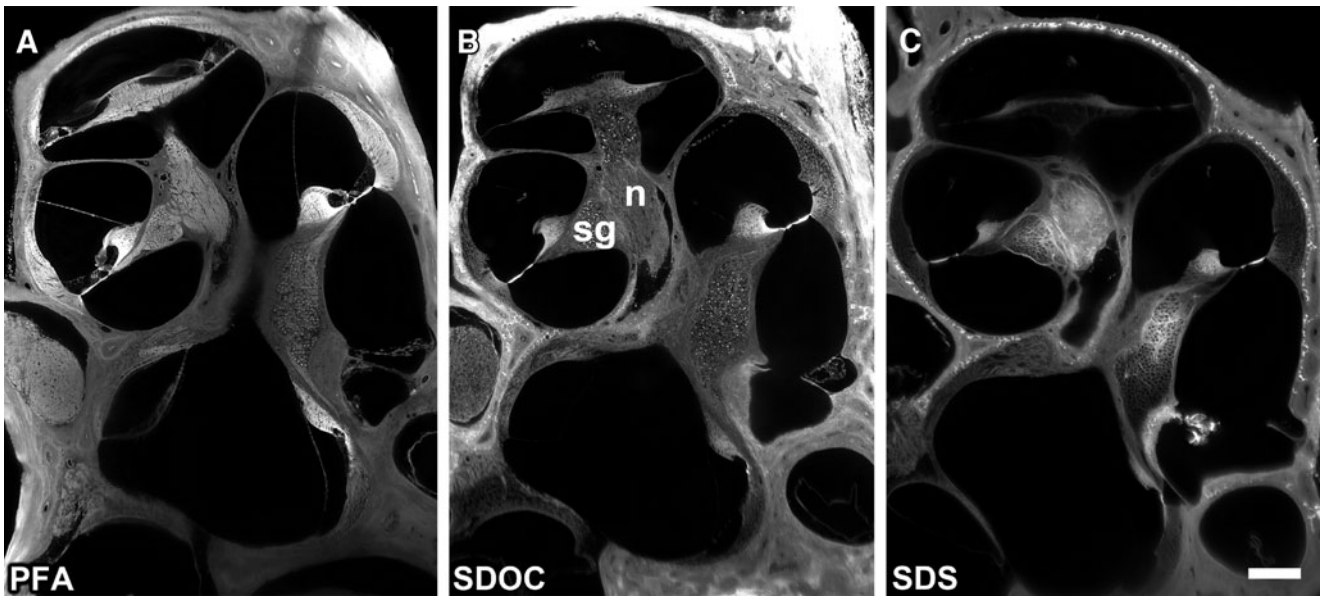

FIG. 1. **A** A midmodiolar sTSLIM optical section through a paraformaldehyde-fixed cochlea showing the full complement of cells and connective tissues of the cochlea. **B** An SDOC decellularized cochlea, showing removal of most cells. However, cell debris were present (bright structures) in the spiral ganglion neurons (*sg*) and modiolar nerve (*n*). **C** After SDS detergent extraction, all cells appear to have been removed from the membranous tissues of the cochlea and spiral ganglion neurons appeared as hollow spheres. Bone lacunae and the basilar membrane are strongly autofluorescent. *Bar*=200 μm.

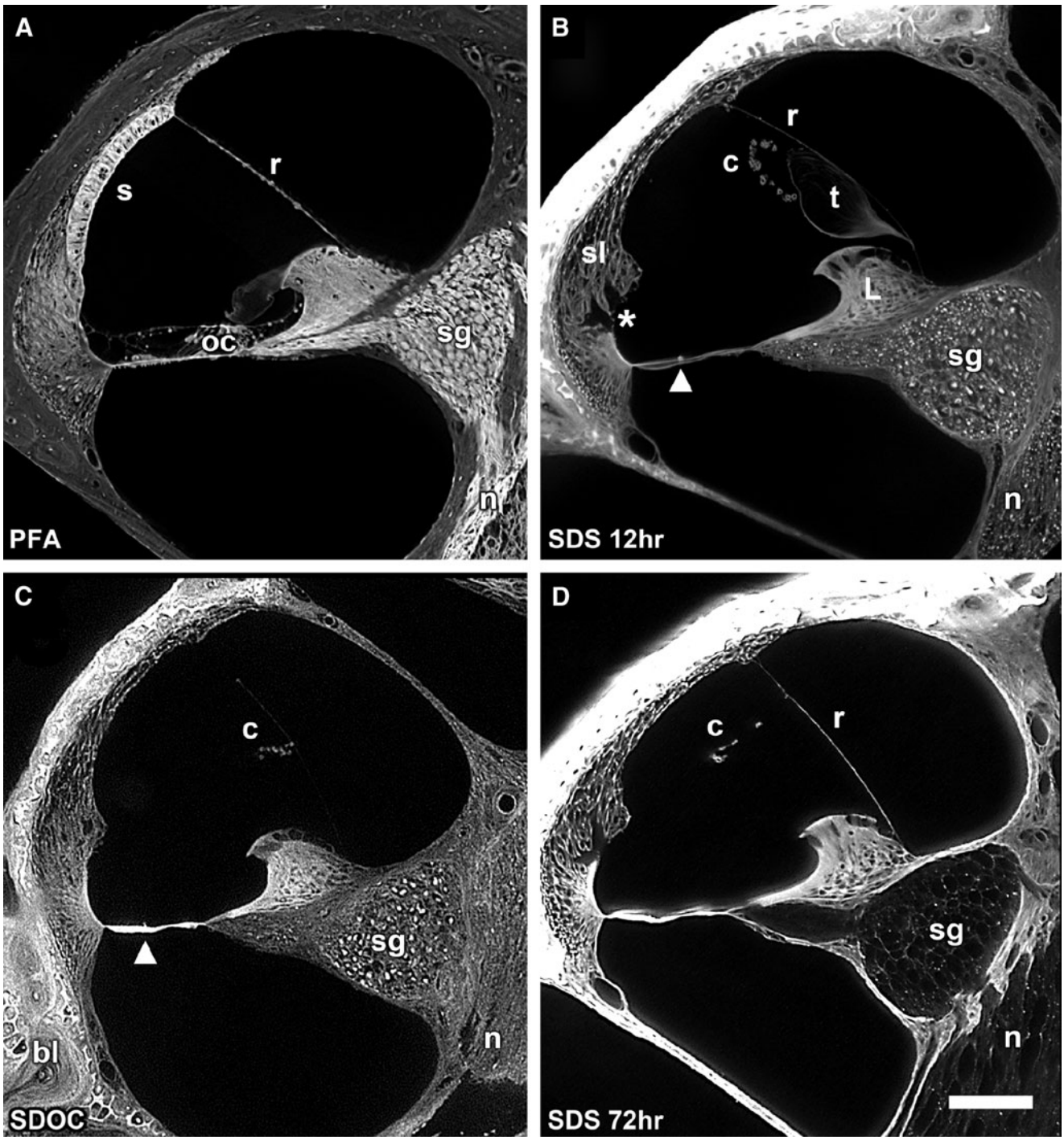

FIG. 2. **A** Paraformaldehyde-fixed cross-section of the scala media showing cells of the basilar membrane including the organ of Corti (*oc*), stria vascularis (*s*), Reissner's membrane (*r*), spiral ganglion neurons (*sg*), and nerves (*n*). **B** A cochlea that was decalcified in SDS for 12 h but not perilymphatically perfused with the detergent. Note the acellular appearance of the spiral ligament (*sl*), removal of the external sulcus cells (*asterisk*), removal of all of the cells of the basilar membrane including the organ of Corti, and the interdental cells of the limbus (*L*). Conical-shaped structures are apparent on the basilar membrane (*arrowhead*). Cells of the stria vascularis have dissolved but its laterally linked capillary network of BL (*c*) remains and appears to "float" within the endolymphatic space. Reissner's membrane persists as a thin BL (*r*). The tectorial membrane (*t*) has lifted off of the limbus and appears to be "floating" as well. Cell debris (bright spots) are present within the sg and n. **C** 72 h SDOC-treated scala media showing cell debris in the sg and n. The basilar membrane structures are present (*arrowhead*). **D** Perilymphatic perfusion with SDS and immersion for 72 h resulted in complete removal of the cells of the scala media and persistence of the ECM, including the spiral ligament, basilar membrane, limbus, stria vascularis *c*, and the BL of r. *Bar*=100 μm.

perilymphatic perfusion of the detergent. Although most cells have been removed, cell debris (bright structures) are present within the ECM surrounding the spiral ganglion neurons and nerves. The spiral ligament is acellular and holes are present in the ligament where the root processes of the external sulcus cells were located. Notice also that the stria vascularis has been dissolved and is no longer attached to the spiral ligament; however, its laterally linked BL of its capillaries appear to be "floating" within the endolymphatic space. The tectorial membrane was separated from the limbus and appears to be "floating" as well. The organ of Corti was removed as well as the interdental cells of the spiral limbus. Reissner's membrane persists only as a thin BL as both of its cell layers were removed. In addition, a novel, prominent series of spirally directed structures have been revealed on the endolymphatic surface of the basilar membrane in decellularized cochleas (Fig. 2B, arrowhead). Even with perilymphatic perfusion and 72-h immersion in SDOC, cell debris remained in the spiral ganglion neurons and in the nerves (Fig. 2C). Basilar membrane structures are also shown in Figure 2C. However, after perilyphatic perfusion with SDS and 72 h of immersion, all cells were removed from scala media tissues including the spiral ganglion neurons and nerves (Fig. 2D). Figure 3 is a higher magnification of the scala media after SDS decellularization and 72 h of immersion in SDS. It shows removal of all cellular components from the nerves and ganglion cells leaving their appearance as hollow tubes and spheres, respectively. Figure 3 insert shows cell debris within the spiral ganglion neuron cell body after SDOC treatment. The interdental cells and cells of the matrix of the limbus were removed. The basilar membrane is strongly autofluorescent and shows structures on its apical surface. Holes in the spiral ligament beneath the spiral prominence were apparent where the external cell sulcus root processes were located. After decellularization with either detergent, the following ECM structures were present: bone, spiral ligament, spiral limbus, basilar membrane, Reissner's membrane BL (either intact or broken), ECM surrounding the nerves and spiral ganglion neurons, and the BL of vascular elements. Cellular structures that were removed were the cells of Reissner's membrane, the interdental cells, fibrocytes of the spiral ligament, spiral ganglion neuron cell bodies and nerves (exceptions described above), the stria vascularis, inner and outer sulcus cells, cells of the upper and lower surface of the basilar membrane including the organ of Corti, and some osteocytes.

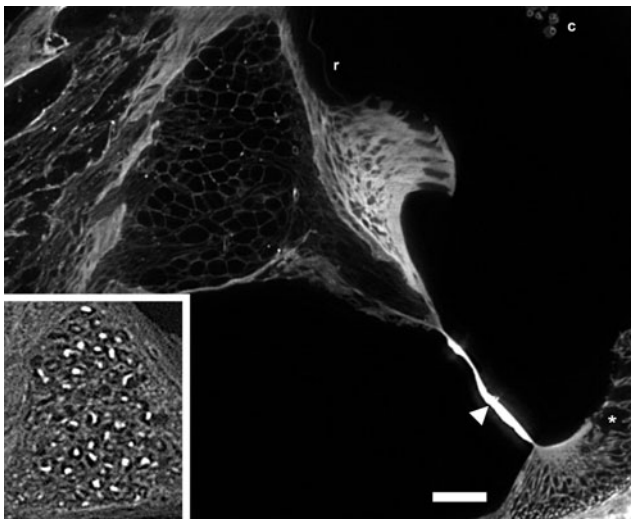

FIG. 3. High-magnification sTSLIM optical section of a mouse cochlea that was decellularized in SDS for 72 h. Spiral ganglion neurons and nerves appear as hollow spheres and tubes, respectively. Basilar membrane structures can also be seen (*arrowhead*), as well as the capillaries of stria vascularis (*c*), the spaces left by the root processes of the outer sulcus cells (*asterisk*) and the thin BL of Reissner's membrane (*r*). *Insert* shows cell debris within the spiral ganglion cell bodies after SDOC treatment (same magnification as the rest of the figure). *Bar*=50 μm.

In order to confirm cell removal, two specific staining procedures were performed: cell and ECM staining by Harris hematoxylin and eosin (H&E) as well as DNA labeling of cell nuclei with SYTOX. Figure 4A–C shows the H&E results in cryosections and photographed using brightfield illumination using an Olympus microscope. The upper panel shows H&E staining in cellularized, and after SDOC and SDS treatment. H&E labeled the cells, their nuclei, and the ECM in paraformaldehyde-fixed normal cochlea (Fig. 4A). After SDOC treatment, only cell nuclei that were labeled were those in the bone of the otic capsule and modiolus, but the ECM was also stained after SDOC (Fig. 4B). After SDS treatment (Fig. 4C), cell nuclei did not appear to be present in the otic capsule and modiolar bone. There was differential staining of the ECM that was detergent dependent with more staining after SDS extraction (Fig. 4C). SYTOX labeled the DNA in all of the nuclei in cellularized cochleas (Fig 5A) but showed little or no labeling of cell nuclei in decellularized cochleas (Fig. 4D). There was no labeling of the ECM in SDOC and SDS decellularized cochleas but cell nuclei that remained in the otic capsule (after SDOC) and other parts of the bone were labeled by SYTOX (Fig. 4E). Decellularization's effect on each scala media tissue is described below.

Bone

The otic capsule was present and many of its osteocytes resisted extraction in SDOC treatment as evidenced by the presence of nuclei (after H&E staining, SYTOX, staining and sTSLIM observations). The lacunae in the

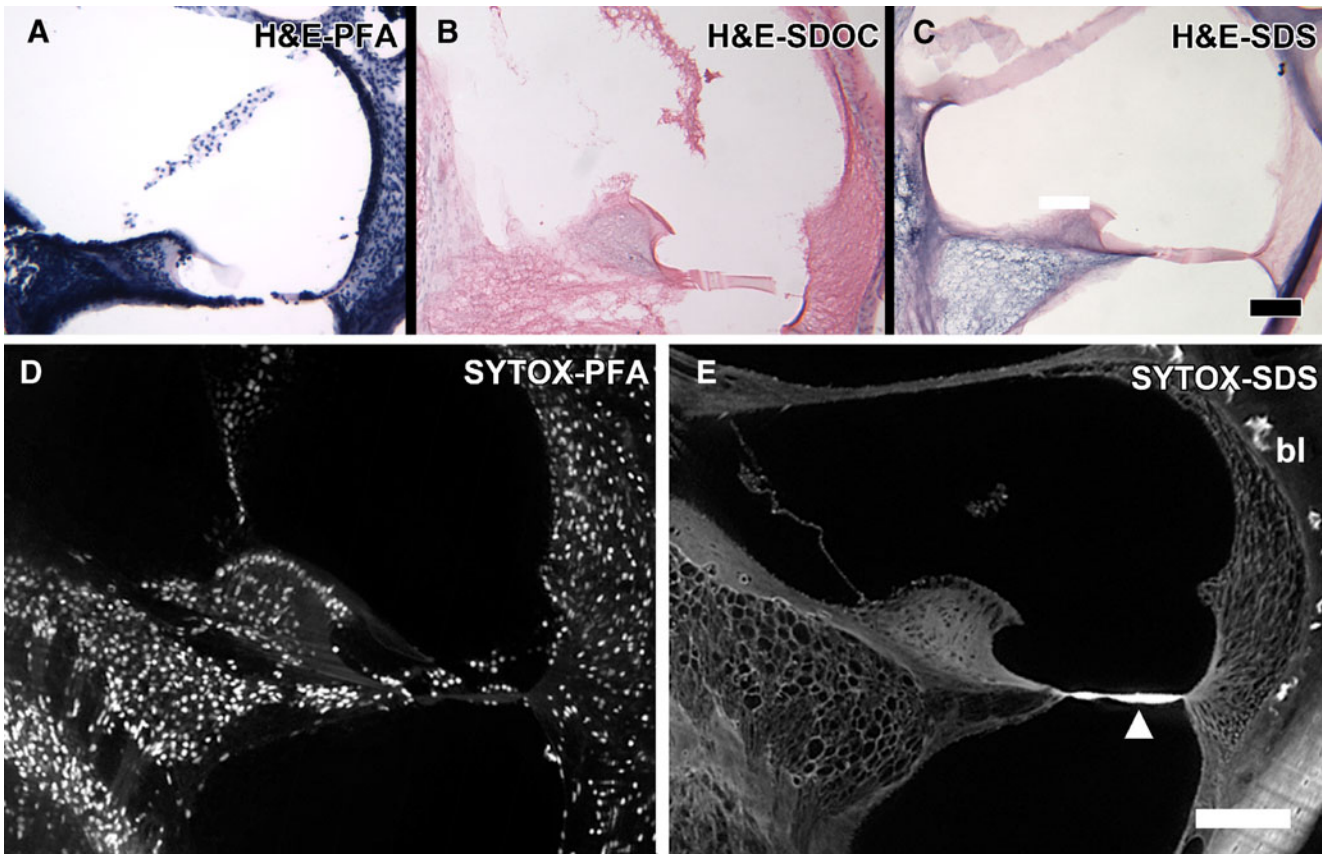

FIG. 4. **A** PFA-fixed mouse cochlea cryosection stained with H&E that shows strong staining of nuclei, cells and ECM. **B** SDOC decellularized scala media cryosection H&E stained showing eosin staining of ECM and nuclei staining in the bone. **C** SDS decellularized scala media cryosection H&E stained showing eosin staining of ECM and diffuse hematoxylin reactivity in the ECM, especially in Rosenthal's canal and the modiolus. Osteocyte nuclei do not appear to be present or labeled in the bone of the otic capsule and modiolus. *Bar*=100 μm D SYTOX-treated paraformaldehyde-fixed, cellularized scala media showing labeling of the DNA in all the cell nuclei. E SYTOX treatment of an SDS decellularized cochlea showing no nuclei labeling. Bone lacunae (*bl*) and the basilar membrane are strongly autofluorescent, and the basilar membrane structures are present here (*arrowhead*). Osteocytes in the otic capsule and modiolus are not present or labeled. *Bar*=100 μm.

otic capsule and the basilar membrane showed strong autofluorescence (Fig. 4E). All of the bone of the cochlea remained after decellularization; however, cell nuclei were present in some of these bones. Osteocytes in the temporal bone adjacent to the annular ligament of the stapes footplate appeared to be the most impervious to detergent extraction (by SDOC and SDS) as they were strongly reactive to SYTOX (not shown).

Basilar membrane and the organ of Corti

The basilar membrane remained attached at its medial and lateral ends and even in Rhodamine unstained tissues, its homogenous matrix showed a strong autofluorescence that gradually diminished toward the cochlear apex (Figs. 1B, C, 2C, D, 3, and 4D). All of its cells, including the organ of Corti as well as its cells above (i.e., Boettcher and Claudius) and below (i.e., mesothelial cells) its homogenous matrix were removed. In addition, there were periodic, acellular structures on the scala media side of the basilar membrane that we had not noticed in fixed tissues. These basilar membrane structures appeared as a series of conical-shaped elevations (5.76 μm±0.15 (SEM) in height and diameter) spaced approximately 25 μm apart that extend spirally along the basilar membrane toward the apex where their distribution became sparse, ending around 70 % of the distance from base to apex (Figs. 1B, C, 2B, D, 3, 4B, and 5A–D). Volume rendering (Fig. 5A, B, and D) of sTSLIM optical sections show the distribution of these structures along the basilar membrane and they also occur in the rat cochlea (Fig. 5D). Figure 5B shows the radial distribution of these structures, which lie between Boettcher and Hensen cells. These structures also appear in paraformaldehyde-fixed cellularized cochleas, but they are not as noticeable due to the surrounding cell processes (Fig. 5C).

Spiral ligament

The spiral ligament appeared relatively unchanged in gross appearance but its cells were removed. The spiral

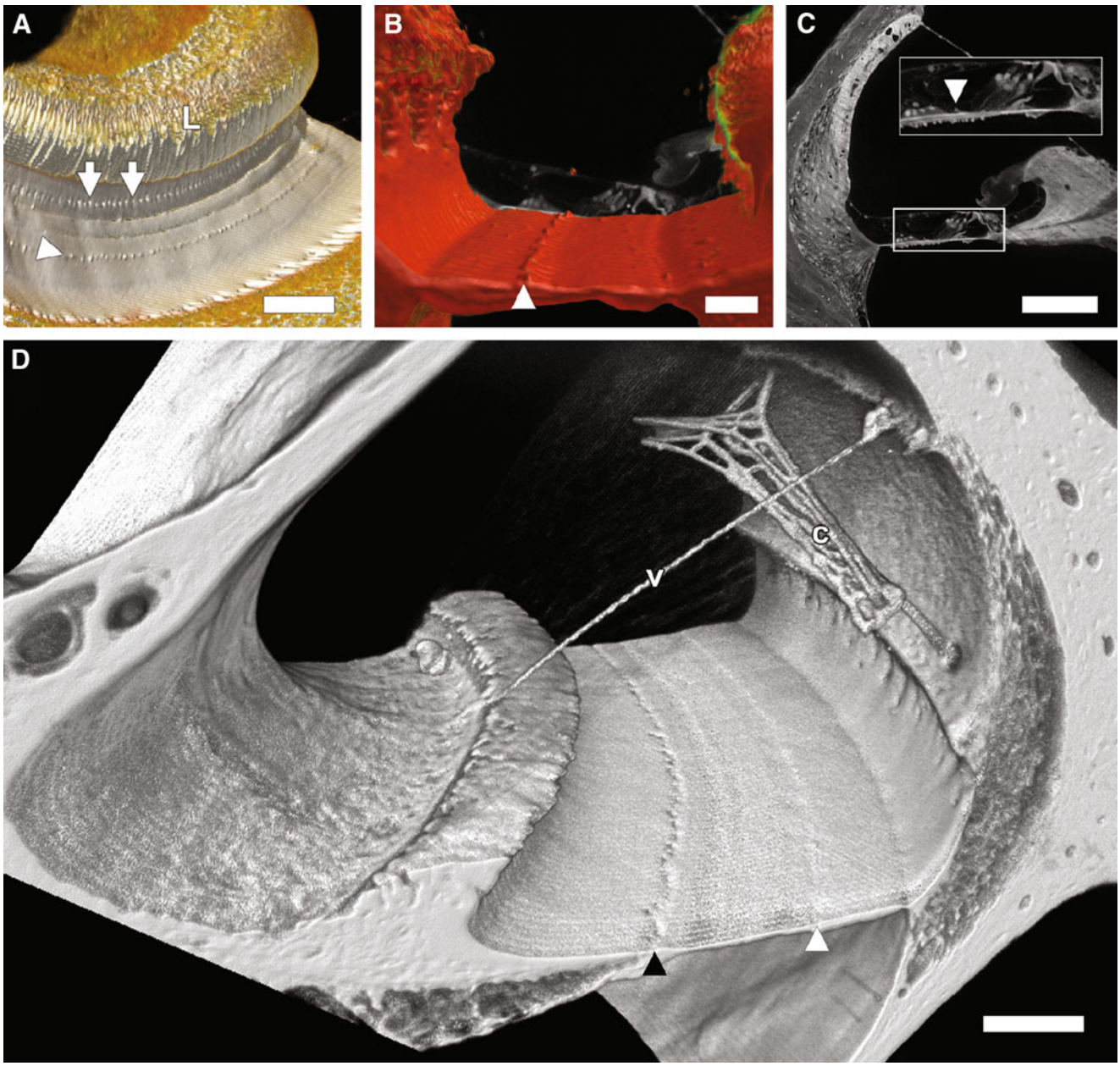

FIG. 5. **A** A direct volume rendering of a portion of the scala media in an SDS-treated cochlea showing the limbus (*L*), habenula perforata (*arrows*), and the basilar membrane structures (*arrowhead*). *Bar*= 100 µm. **B** An overlay of a cellularized (in the background) and decellularized scala media orthogonal cross-section showing the location of the structures (*arrowhead*) between Boettcher and Hensen cells. Bar=50 µm. **C** Scala media cross-section from a paraformaldehyde-fixed cochlea shows what appears to be the structures (*arrowhead*) among the cells overlying the basilar membrane. *Bar*=100 µm. **D** A direct volume rendering of a portion of the scala media from an SDS-treated rat cochlea. Cell removal is obvious and most of the stria vascularis BL capillary network (*c*) is detached from the spiral ligament except at two locations. Vessel BL (*v*) was also observed traversing Reissner's membrane which is not present. The habenula perforata are visible as a series of depressions running along the basilar membrane (*filled arrowhead*). Spirally arranged basilar membrane structures are indicated by the *white arrowhead*. *Bar*=50 µm.

prominence and the basilar crest remained but the external sulcus cells and their root process were removed, and the root processes left holes in the spiral ligament (Fig. 2B, D; Supplemental movie 1 in the Electronic supplementary material (ESM)). The stria vascularis was not present on the endolymphatic surface of the spiral ligament.

Stria vascularis

Cells of the stria vascularis were removed and the only part of this tissue that remained was the laterally linked BL of its capillaries and associated vessels (Figs. 2B, D and 3A). Portions of this capillary network were still attached to the spiral

ligament by the radiating arterioles and collecting veins BL in the mouse and in the rat (Fig. 5). However, over most of the length of the scala media, this capillary network appeared to "float" within the scala media and lodge near Reissner's membrane BL. In the rat cochlea, a vessel BL was also seen traversing Reissner's membrane (Fig. 5D).

Reissner's membrane

In several cochleas treated with detergent, Reissner's membrane was recognized as an acellular BL that remained attached at the spiral ligament and the spiral limbus (Figs. 1C and 2B, C). In other parts of the cochlea and in other animals, it was detached at its spiral ligament end but fragments of it remained attached at its spiral limbus end (Figs. 3B).

Spiral limbus

The spiral limbus appeared somewhat enlarged and had apical holes that were created by the removal of the interdental cells (Fig. 2B–D and 3B). BL of vascular elements and stromal cells were present in the limbus but the cells of the inner sulcus cells were absent.

Tectorial membrane

In shorter (i.e., 12 h) detergent incubation times, the tectorial membrane was present and lifted up from the spiral limbus (Fig. 2B). In longer incubation times (i.e., 72 h) it was detached from the spiral limbus and was either flushed completely out of the scala media or it lodged in another part of the endolymphatic space by the perilymphatic perfusion of the decellularization solutions. The tectorial membrane appeared similar to its unfixed state after decellularization and was not shrunken as it appears after fixation and dehydration (Figs. 1A, 2A, 3A, D, and 5C).

Rosenthal's canal and spiral ganglion neurons

With short incubation times and after SDOC treatment, the ECM surrounding the spiral ganglion neuron cell bodies and nerves contained autofluorescent cell debris (Figs. 1B and 2B, C). However, after 72 h of SDS treatment, spiral ganglion neuron cell bodies appeared as hollow spheres surrounded by ECM (Figs. 2D, 3, and 4B) and their nerves appeared as hollow tubes (not shown).

Human temporal bone

Figure 6A–C shows a normal formalin-fixed human temporal bone and a fresh, unfixed decellularized temporal bone that were imaged by TSLIM and sTSLIM respectively. Figure 6A, that was imaged by TSLIM, shows streaking artifacts produced by the static light-sheet of TSLIM imaging but normal morphology of the cells and tissues of the scala media including the stria vascularis and the organ of Corti. Figure 6B shows removal of cells from the human cochlea by SDS decellularization. Stria vascularis BL appear to "float" within the endolymphatic space and the cells of the spiral ligament, limbus, and basilar membrane were removed. Basilar membrane structures were present but seem more numerous than in the mouse or rat. Figure 6C is a volume rendering of the decellularized human scala media and shows the stria capillary BL, spiral prominence, basilar membrane structures, but no holes are seen where the external cell root processes that were removed were observed in the mouse and rat cochleas.

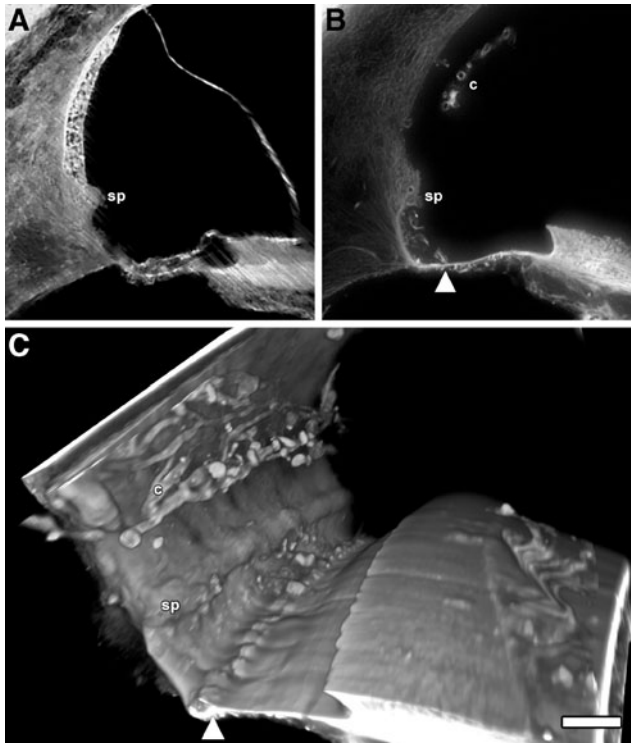

FIG. 6. **A** ATSLIM scala media cross-section from a normal, formalin-fixed human temporal bone showing typical cells and tissues including the spiral prominence (*sp*). **B** SDS decellularized human temporal bone cross-section showing decellularization of scala media structures, a free-floating capillary network of the stria vascularis (*c*), the *sp* and what appears to be structures (*arrowhead*) on basilar membrane at a similar in location as was found in the mouse and rat. Note that there are no external sulcus cell holes in the spiral ligament similar to that which was observed in the mouse and rat. **C** A direct volume rendering of the scala media showing the BL of the c and sp and the basilar membrane structures (*arrowhead*). *Bar*=100 μm.

Immunohistochemistry

After whole cochlea SDS decellularization, decalcification, perilymphatic perfusion with antibodies

against laminin and type IV collagen and subsequent perfusion with a fluorophore labeled secondary antibody, these glycoconjugates were revealed (Fig. 7). Cryosections of SDOC tissues immunolabeled for laminin and type IV collagen showed a similar distribution of these glycoconjugates (not shown) compared with the sTSLIM observations. Figure 7A shows an sTSLIM section after laminin labeling. Vascular BL are labeled as well as a few epithelial BL (basilar crest) and neural BL. Type IV collagen antibody labeling was similar to the laminin labeling with the same vascular, epithelial and neural BL labeled. Figure 7C is a volume rendering of type IV collagen labeling. One can actually trace a radiating arteriole entering a stria capillary and the collecting venule leaving the strial capillary network. Notice

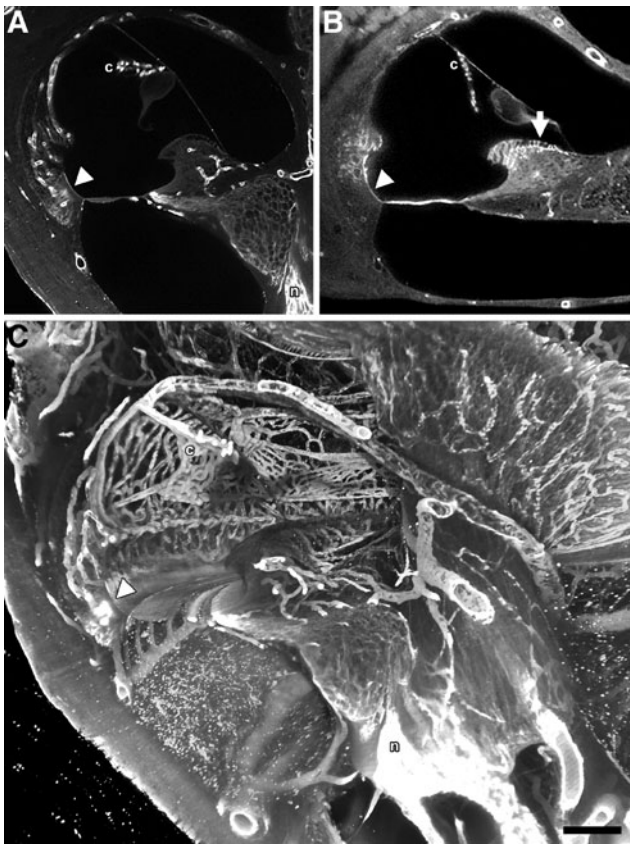

FIG. 7. **A** sTSLIM optical section showing type IV collagen labeling of the BL of the capillaries of the stria vascularis (*c*), BL of the basilar crest (*arrowhead*) and the nerves (*n*). **B** sTSLIM optical section showing laminin labeling of the BL of the capillaries of the c, BL of the basilar crest (*arrowhead*) and BL of the interdental cells (*arrow*). **C** Direct volume rending of 50 midmodiolar sections from a collagen IV antibody-labeled, 72-h SDS-treated cochlea. Image represents a 250-µm-thick (*z*-dimension) volume rendering from the center of the specimen. The collagen IV antibody labeled BL in the decellularized capillaries of c, vas spirale, large vessels of the scala tympani and modiolus, spiral limbus and spiral ligament, basilar crest epithelial BL (*arrowhead*) as well as the antibody accessible ECM of the cochlear *n*. Also note that, that the scala tympani vessels appear to lie inside the scala, but they are actually encased in thin bone. *Bar*=200 µm.

labeling of the vas spirale, epithelial BL of the basilar crest and nerves and large vessels within the bone of the scala tympani. A movie showing whole cochlea labeling by type IV collagen antibodies is available (Supplementary movie 2 in the ESM).

Vestibular

Macula and crista ampullaris

sTSLIM cross-section of the crista ampullaris in cellularized tissues (Fig. 8A) contained hair cells and supporting cells in the saddle shaped ridge of ECM. After SDS extraction, only the ECM core (Fig. 8B) and the underlying BL of the nerves were present. The acellular crista ampullaris appeared "spiky" due to removal of the hair cells and supporting cells. The saccule from a paraformaldehyde fixed cellularized cochlea (Fig. 8C) showed the macula with hair cells and supporting cells and the BL of underlying nerves. After SDS treatment, the macula (Fig. 8D) was devoid of cells and only the ECM and BL of the underlying nerves remained. Scarpa's ganglion cells and their processes appeared as hollow spheres and tubes respectively after decellularization as was observed for the spiral ganglion neurons.

DISCUSSION

Unfixed, decellularized ear tissues were compared with normal, cellularized paraformaldehyde fixed tissues. All tissues were treated with EDTA to remove calcium, ethanol to remove water and lipids, and MSBB to clear tissues to transparency. Detergent extraction was only successful on fresh, unfixed tissue. Osteocytes were better extracted with SDS vs. SDOC and those that were most resistant were those of the annular ligament. This is probably due to bone density and the inaccessibility of the detergents to penetrate the bone. In addition, spiral ganglion neurons within Rosenthal's canal and modiolar nerves were also difficult to completely decellularize. This is presumably due to poor diffusion of the detergents and removal of cellular extracts through dense bone of Rosenthal's canal and the modiolus. SDS treatment by perilymphatic perfusion and 72-h immersion was the only detergent that removed the cellular components of the spiral ganglion neurons and nerves. However, we only tried extraction for 12 and 72 h, so a longer extraction time with SDOC may succeed in complete cellular extraction. Cell solubilization products appear to diffuse through soft tissues of the cochlea as evidenced by the presence of cloudy effluents exiting the cochlea during perilymphatic perfusion. Although SDS decellularization produced

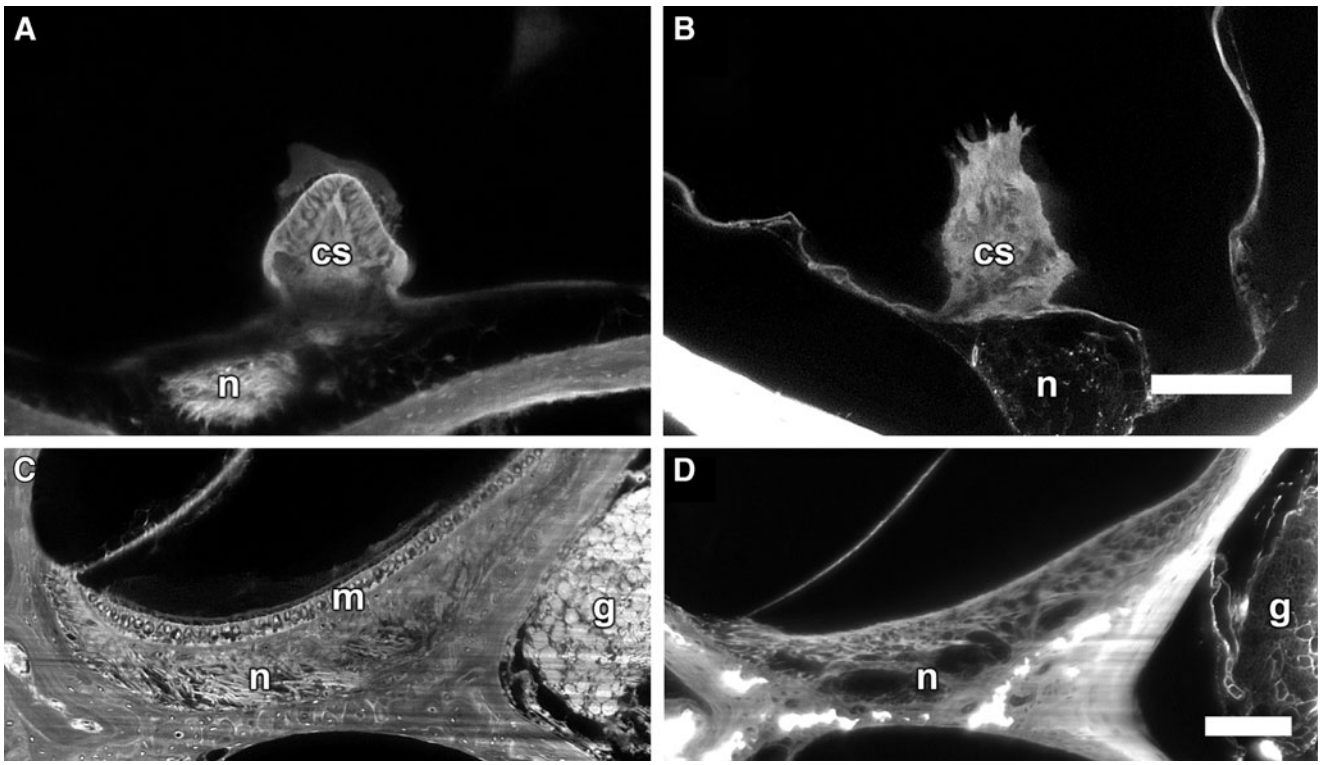

FIG. 8. Vestibular system. **A** A paraformaldehyde-fixed normal mouse ampulla of a semicircular canal showing the crista ampullaris with hair cells and supporting cells (*cs*) embedded in the saddle-shaped ECM with nerves (*n*). **B** A cross-section through the ampulla in an SDS-treated animal showing a "spiky" appearance with extraction of the hair and supporting cells and with only the ECM remaining and BL of the *n*. *Bar*=100 μm (**A**, **B**). **C** A cross-section of the saccule from a paraformaldehyde-fixed cellularized mouse cochlea showing the macula with hair cells and supporting cells (*m*), and underlying g and n. **D** A cross-section of the saccule from an SDS-treated animal showing dissolution of the cells of the macula and the extraction of cell components from the g and n. *Bar*=100 μm (**A**, **B**).

hollow spheres and tubes of BL of the spiral ganglion neurons and seem to be ideal for engraftment by stem cells, it appears that SDS treatment removes more cellular components compared with SDOC. Although it is unknown which ECM components in decellularized cochleas would induce stem cells to an auditory phenotype, SDOC may be preferable to SDS decelullarization for stem cell engraftment since it appears to extract less cellular components. Future experiments will reveal if this is true. However, laminin and type IV collagen were present after both detergent extractions. It is reasonable to expect that SDS solubilizes glycoproteins and collagens as it is a standard protocol for protein solubilization for Western immunoblotting. However, we used this protocol on the cochlea since it worked so well for heart decellularization and myocyte engraftment (Ott et al. 2008). Decellularization protocols may have to be optimized for different tissue types and their purpose, such as for ECM differentiation of stem cells or organ transplantation. For stem cell differentiation, it may not be necessary or desirable to extract all cell components; however, this is a critical requirement for organ transplantation to avoid cellular-based immunologic rejection of the transplant.

After decellularization it was striking to see how much of the membranous labyrinth is ECM and remained without any tissue fixation. The anatomical boundaries of the scala media are still well defined with the BL of Reissner's membrane, the spiral ligament and the basilar membrane forming the triangle-shaped tissue of the cochlear duct. Since cells and their tight juctions are removed, these decellularized cochlear preparations are very permeable and might be useful for investigating the passive fluid and mechanical properties of the scala media. We have shown that these preparations are also permeable to whole cochlea, antibody labeling of ECM components (e.g., laminin and type IV collagen) that could not be labeled in whole, fixed, cellular tissue.

The ECM of the basilar membrane appeared relatively unchanged and remained attached at its medial and lateral ends. It also exhibited a graded decrease in autofluorescence from its base to apex, which may be related to its stiffness gradient. We have previously reported the presence of fibronectin, tenascin, and type II collagen in the homogenous ground substance of the basilar membrane (Santi et al. 1989; Tsuprun and Santi 1999), and it remains to be seen whether these materials are present in the

decellularized cochleas. The BL of Reissner's membrane seems to be strong, since it remained in cochleas that were perilymphatically perfused with detergents. In addition, when detached, it was at its limbal rather than spiral ligament end, suggesting this end may be a stronger attachment. Although the lateral intermingling of ECM connections of the capillaries of the stria vascularis has been known for some time, it was impressive to see how these BLs held on to one another when all of the surrounding cells were removed. This stria vascularis capillary BL complex might make an interesting in vitro preparation for investigating the properties of strial capillary ECMs. The basilar membrane spirally directed structures that were so prominent in decellularized cochleas may be a new observation. These structures occur in the mouse, rat, human and probably in other animals as well. It is not completely clear what these structures are. Their location seems to be the lateral edge of Hensen's cells and the medial edge of Boettcher cells. They seem to be extracellular as they persist after all the cells of the basilar membrane have been removed. Thus, it is unlikely that they are composed of tubulin, which occurs in the base of Hensen's cells. They could be extensions of ECM of the basilar membrane, but their structure and function remain unclear.

With removal of the interdental cells of the limbus and the organ of Corti, the tectorial membrane appeared to "float" within the endolymphatic space and since its attachment to the limbus and organ of Corti were dissolved, it was often flushed out or lodged in other parts of the cochlea. It is not clear whether the detergents altered its anatomy since these cochleas were not fixed. After conventional fixation, decalcification and dehydration shrinkage of the tectorial membrane is obvious, but after decellularization, decalcification and dehydration the tectorial membrane exhibit an unfixed morphology. Again, this free floating tectorial membrane might be useful for in vitro isolated preparation experiments.

Our original purpose in decellularizing fresh cochleas was to allow access of anti-matrix antibodies to infiltrate and label ECM components in whole cochleas for sTSLIM imaging. Laminin and type IV collagen antibodies exhibit robust staining of the ECMs in several tissues of decellularized cochleas. Both glycoconjugates appears in vascular tissues and to a lesser extent in neural and epithelial BL as well. It will be interesting to determine which other ECM components, like fibronectin, tenascin, heparan sulfate, and collagens (type II) have survived detergent decellularization.

The protocols that we used to produce acellular cochleas were obtained from investigators who successfully use decellularized tissues as superior 3D matrices (compared with synthetic matrices) to induce, engraft, and differentiate stem and other progenitor cells for producing transplantable organs. For example, Ross et al. (2009) used decellularized kidney scaffolds and seeded them with pluripotent murine embryonic stem cells. After decellularization with SDS, acellular kidneys became transparent yet retained the web-like appearance of the BL architecture like we observed with decellularized cochlea. The kidney BL contained laminin and type IV collagen, which we also demonstrated in decellularized cochleas. After seeding, kidney cells lost their embryonic appearance and proliferated within the glomerular, vascular and tubular structures of the kidney. Some organs may be grown in vitro using cells for an autologus (cells from the host) transplant, and since foreign cells were removed, the patient would not require immunosuppresive drug treatment. A transplantable cochlea does not seem to be a possibility; however, it seems reasonable that stem cells could be grown and directed toward an auditory phenotype on decellularized cochlear tissue, since the 3D geometry and many ECM components remain in these acellular preparations as provided by nature. These partially differentiated cells could be released from the ECM in vitro and injected into damaged cochlea in vivo for engraftment and differentiation in order to restore function. We are working to determine if stem cells will recognize ECM components in decellularized cochlear tissue and can be directed to an auditory phenotype. If successful, induced autologous stem cells may become a useful as a new approach for providing cochlear and vestibular cell regeneration in order to restore function in damaged ears.

ACKNOWLEDGMENTS

The authors acknowledge the assistance by Sebahattin Cureoglu, Monika Schachern, and Meredith Adams for human temporal bone processing. Funding was provided to PAS by the NIDCD (RO1DC007588-04), an ARRA supplement (RO1DC007588-03S1), human temporal bone processing by NIDCD (U24DC011968-01), the Capita Foundation, and the Lions Hearing Foundation.

REFERENCES

BAIGUERA S, JUNGEBLUTH P, BURNS A, MAVILIA C, HAAG J, DE COPPI P, MACCHIARINI P (2010) Tissue engineered human tracheas for in vivo implantation. Biomaterials 33:780–789

CORRALES CE, PAN L, LI H, LIBERMAN MC, HELLER S, EDGE ASB (2006) Engraftment and differentiation of embryonic stem cell-derived neural progenitor cells in the cochlear nerve trunk: growth of processes into the organ of Corti. J Neurobio 66:1489–1500

Crapo PM, Gilbert TW, Badylak SF (2011) An overview of tissue and whole organ decellularization processes. Biomaterials 32:3233–3243

Erdbrügger W, Konertz W, Dohmen PM, Posner S, Ellerbrok H, Brodde OE, Robenek H, Modersohn D, Pruss A, Holinski S, Stein-Konertz M, Pauli G (2006) Decellularized xenogenic heart valves reveal remodeling and growth potential in vivo. Tissue Eng 12:2059–2068

Evans A, Euteneuer S, Chavez E, Mullen L, Hui E, Bhatia S, Ryan A (2007) Laminin and fibronectin modulate inner ear spiral ganglion neurite outgrowth in an in vitro alternate choice assay. Bev Neurobiol 67:1721–1730

Gilbert TW, Sellaro TL, Badylak SF (2006) Decellularization of tissues and organs. Biomaterials 27:3675–3683

Hori R, Nakagawa T, Sakamoto T, Matsuoka Y, Takebayashi S, Ito J (2007) Pharmacological inhibition of Notch signaling in the mature guinea pig cochlea. Neuroreport 18:1911–1914

Hynes RO (2009) The extracellular matrix: not just pretty fibrils. Science 326:1219–1261

Iguchi F, Nakagawa T, Tateya I, Kim TS, Endo T, Taniguchi Z, Naito Y, Ito J (2003) Trophic support of mouse inner ear by neural stem cell transplantation. Neuroreport 14:77–80

Izumikawa M, Minoda R, Kawamoto K, Abrashkin KA, Swiderski DL, Dolan DF, Brough DE, Raphael Y (2005) Auditory hair cell replacement and hearing improvement by *Atoh1* gene therapy in deaf mammals. Nat Med 11:271–276

Kesser BW, Lalwani AK (2009) Gene therapy and stem cell transplantation: strategies for hearing restoration. Adv Otorhionlaryngol 66:64–86

Khan SA, Nelson MS et al (2008) Endogenous heparan sulfate and heparin modulate bone morphogenetic protein-4 signaling and activity. Am J Physiol Cell Physiol 294:C1387–C1397

Lang H, Schulte BA, Goddard JC, Hedrick M, Schulte JB, Wei L, Schmiedt RA (2008) Transplantation of mouse embryonic stem cells into the cochlea of an auditory-neuropathy animal model: effects of timing after injury. JARO 9:225–240

Löwenheim H, Furness DN, Kil J, Zinn C, Gültig K, Fero ML, Frost D, Gummer AW, Roberts JM, Rubel EW, Hackney CM, Zenner HP (1999) Gene disruption of p27K(Kip1) allows cell proliferation in the postnatal and adult organ of Corti. PNAS 96:4048–4088

Martinez-Monedero R, Corrales CE, Cuajungco MP, Heller S, Edge AS (2006) Reinnervation of hair cells by auditory neurons after selective removal of spiral ganglion neurons. J Neurobiol 66:319–331

Nagao RJ, Lundy S, Khaing ZZ, Schmidt CE (2011) Functional characterization of optimized acellular peripheral nerve graft in a rat sciatic nerve injury mode.l. Neurol Res 33:600–608

Nayagam B, Minter RL (2011) A comparison of in vitro treatments for directing the differentiation of stem cells towards a sensory neural fate. Am J Otol 33:37–46

Oshima K, Shin K, Diensthuber M, Peng AW, Ricci AJ, Heller S (2010) Mechanosensitive hair cell-like cells from embryonic and induced pluripotent stem cells. Cell 141:704–716

Ott HC, Matthiesen TS, Goh SK, Black LD, Kren SM, Netoff TI, Taylor DA (2008) Perfusion-decellularized matrix: using nature's platform to engineer a bioartificial heart. Nat Med 14:213–221

Petersen TH, Calle EA, Zhao L, Lee EJ, Gui L, Raredon MB, Gavrilov K, Yi T, Zhuang ZW, Breuer C, Herzog E, Niklason LE (2010) Tissue-engineered lungs for in vivo implantation. Science 329:538–541

Ross E, Williams M, Hamazaki T, Terada N, Clapp W, Adin C, Ellison G, Jorgensen M, Batich C (2009) Embryonic stem cells proliferate and differentiate when seeded into kidney scaffolds. J Am Soc Nephrol 20:2338–2347

Santi PA, Larson JT, Furcht LT, Economou TS (1989) Immunohistochemical localization of fibronectin in the chinchilla cochlea. Hear Res 39:91–101

Santi PA, Johnson SB, Hillenbrand M, GrandPre PZ, Glass TJ, Leger JR (2009) Thin-sheet laser imaging microscopy for optical sectioning of thick tissues. Biotechniques 46:287–294

Schröter TJ, Johnson SB, John K, Santi PA (2012) Scanning thin-sheet laser imaging microscopy (sTSLIM) with structured illumination and HiLo background rejection. Biomedical Opt Express 1:170–177

Tsuprun V, Santi PA (1999) Ultrastructure and immunohistochemical identification of the extracellular matrix of the chinchilla cochlea. Hear Res 129:35–49